# Radical-like Behavior of Manganese Oxide Cation in Its Gas-Phase Reactions with Dihydrogen and Alkanes

**Matthew F. Ryan, Andreas Fiedler, Detlef Schröder, and Helmut Schwarz***

*Contribution from the Institut für Organische Chemie der Technischen Universität Berlin, Strasse des 17. Juni 135, D-10623 Berlin, Germany*

*Received September 9, 1994*[⊗]

**Abstract:** The gas-phase ion–molecule reactivity of $MnO^+$ with dihydrogen and small alkanes has been examined by using Fourier transform ion cyclotron resonance mass spectrometry. $MnO^+$ was produced from the reaction of laser-desorbed $Mn^{+}$* with $N_2O$. Thermalized $MnO^+$ reacts very efficiently ($k_R = 2.3 \times 10^{-10}$ cm$^3$ molecule$^{-1}$ s$^{-1}$) with $H_2$ to eliminate either a H$^\bullet$ radical or $H_2O$ from the collision complex; both reactions commence with H-atom abstraction. Similarly, H-atom abstraction predominates in the reaction of $MnO^+$ with methane ($k_R = 5.1 \times 10^{-10}$ cm$^3$ molecule$^{-1}$ s$^{-1}$) with a small fraction of methanol being formed. In the reaction of $MnO^+$ with ethane also $\beta$-hydrogen transfer to yield water and ethene as neutral products takes place, and for alkanes larger than ethane, formation of $MnOH(olefin)^+$ products is also observed; the latter reaction is suggested to occur through an initial hydrogen-abstraction process followed by metal-induced C–C bond cleavage. For the $MnO^+$/propane system, ligand exchange reactions were applied to characterize the product formed via $CH_3^\bullet$ loss, which exhibits a $(C_2H_4)MnOH^+$ structure rather than that of an alkoxide, i.e., $Mn(OC_2H_5)^+$. In order to evaluate the electronic ground state of $MnO^+$ and $MnOH^+$, ab initio MO calculations have been performed. At the CASPT2D level of theory, $MnO^+$ exhibits a $^5\Sigma^+$ ground state with a very closely spaced $^5\Pi$ state. For $MnO^+$ the computed bond dissociation energy (BDE) of 65 kcal/mol compares well with the experimental figure of 68 kcal/mol. For $MnOH^+$ the calculations reveal a $^6A'$ ground state with BDE($Mn^+$–OH) = 74 kcal/mol; the experimental value amounts to 81 ± 4 kcal/mol.

## Introduction

Higher oxides of manganese, such as $MnO_2$ and $MnO_4^-$, are versatile oxidation agents that are frequently employed in organic synthesis.[1] For example, $MnO_2$ is used to oxidize allylic and benzylic alcohols to the corresponding carbonyl compounds, to dehydrogenate cyclic compounds to arenes, and to catalyze the C–C bond cleavage of glycols. Permanganate serves to convert olefins to diols, ketones, and carboxylic acids under mild conditions. Furthermore, $MnO_4^-$ allows the oxidation of methylarenes to aromatic carboxylic acids. An interesting aspect is to probe the potential of manganese oxides as oxidants for *saturated* hydrocarbons. The conversion of hydrocarbons, particularly the selective oxidation of methane to methanol, is one of the most significant challenges scientists are faced with today.[2]

Reactivity studies of bare transition-metal ions with hydrocarbons have provided a wealth of insight concerning the intrinsic interactions of metal ions with organic substrates.[3] In particular, mass spectrometric methods and ion beam techniques have uncovered the origins of C–H and C–C bond activation in numerous processes mediated by bare transition-metal cations. Parallel to the reactivity studies, the foundation of thermochemical data regarding $M^+$–L bond strengths continues to grow,[4,5] thus providing a prerequisite for a classification of transition-metal-mediated reactions. Furthermore, the application of theoretical methods afforded significant progress with respect to bonding and reactivity problems. In particular, the combination of experimental and theoretical approaches has been extremely beneficial toward understanding and interpreting the reaction mechanisms and periodic trends in gas-phase transition-metal ion chemistry.[6,7]

Although most of the bare transition-metal cations are able to activate C–H and C–C bonds of larger alkanes (RH),[3] the bare ground-state manganese cation remains an exception in that it does not react with alkanes.[8] This inertness has been ascribed to the high-spin ground state of $Mn^+$ ($^7S$).[9] Specifically, the repulsive character of the 4s orbital in the half-filled ($3d^54s^1$) valence shell for the ground-state $Mn^+$ configuration destabilizes the $Mn^+$(RH) encounter complexes. Therefore, the dissociation energies of $Mn^+$(RH) complexes are much lower as compared to other first-row transition-metal cations.[10] For example, Weisshaar and co-workers[9,10] have reported that under multiple-collision conditions, $Mn^+$ undergoes clustering with methane much slower than other bare transition-metal cations,

[⊗] Abstract published in *Advance ACS Abstracts*, February 1, 1995.

(1) (a) March, J. *Advanced Organic Chemistry*, 3rd ed.; John Wiley and Sons: New York, 1985. (b) Arndt, D. *Manganese Compounds as Oxidizing Agents in Organic Chemistry*; Open Court Publishing: La Salley, IL, 1981.

(2) *Chem. Eng. News* **1993**, (May 31), p 27.

(3) (a) Allison, J. *Prog. Inorg. Chem.* **1986**, *34*, 627. (b) Freiser, B. S. *Chemtracts – Anal. Phys. Chem.* **1989**, *1*, 65. (c) Armentrout, P. B. In *Selective Hydrocarbon Activation*; Davies, J. A., Watson, P. L., Liebman, J. F, Greenberg, A., Eds.; VCH Publishers: New York, 1990; p 467. (d) Eller, K.; Schwarz, H. *Chem. Rev.* **1991**, *91*, 1121.

(4) (a) Allison, J.; Mavridis, A.; Harrison, J. F. *Polyhedron* **1988**, *7*, 1573. (b) Armentrout, P. B.; Georgiadis, R. *Polyhedron* **1988**, *7*, 1573.

(5) Martinho-Simões, J. A.; Beauchamp, J. L. *Chem. Rev.* **1990**, *90*, 629.

(6) (a) Schröder, D.; Fiedler, A.; Hrušák, J.; Schwarz, H. *J. Am. Chem. Soc.* **1992**, *114*, 1215. (b) Fiedler, A.; Schröder, D.; Shaik, S.; Schwarz, H. *J. Am. Chem. Soc.* **1994**, *116*, 10734. (c) D. Schröder, H. Schwarz *Angew. Chem., Int. Ed. Engl.*, in press.

(7) For recent examples of theoretical approaches, see: (a) Kawamura-Kuribayashi, H.; Koga, N.; Morokuma, K. *J. Am. Chem. Soc.* **1992**, *114*, 2359. (b) Musaev, D. G.; Koga, N.; Morokuma, K. *J. Phys. Chem.* **1993**, *97*, 4064. (c) Siegbahn, P. E. M.; Blomberg, M. R. A.; Svensson, M. *J. Am. Chem. Soc.* **1993**, *155*, 1952. (d) Perry, J. K.; Ohanessain, G.; Goddard, W. A., III. *J. Phys. Chem.* **1993**, *97*, 5238. (e) Bushnell, J. E.; Kemper, P. R.; Bowers, M. T. *J. Phys. Chem.* **1994**, *98*, 2044. (f) Partridge, H.; Bauschlicher, C. W.; Jr. *J. Phys. Chem.* **1994**, *98*, 2301. (g) Perry, J. K.; Ohanessian, G.; Goddard, W. A., III. *Organometallics* **1994**, *13*, 1870.

(8) (a) Elkind, J. L.; Armentrout, P. B. *J. Phys. Chem.* **1987**, *91*, 2037. (b) Georgiadis, R.; Armentrout, P. B. *Int. J. Mass Spectrom. Ion. Processes* **1989**, *82*, 123.

(9) Tonkyn, R.; Weisshaar, J. C. *J. Phys. Chem.* **1986**, *90*, 2305.

(10) Tonkyn, R.; Ronan, M.; Weisshaar J. C. *J. Phys. Chem.* **1988**, *92*, 92.

0002-7863/95/1517-2033$09.00/0 

and the efficiency $\Phi$ of reaction 1 is as low as $10^{-4}$; here, $\Phi$ defines the ratio of the measured rate constant $k_R$ to the collision frequency $k_C$.[11]

$$Mn^+ + CH_4 \rightarrow Mn(CH_4)^+ \quad (1)$$

With respect to a gas-phase ion−molecule reaction, bond activation of an alkane by bare $Mn^+$ will only occur if the energy demand of the associated transition structure is lower than the binding energy of the encounter complex $Mn(RH)^+$. However, for $Mn^+$ the complexation energies gained upon $Mn(RH)^+$ formation are on the order of only 10 kcal/mol.[10] Furthermore, bond activation frequently involves R−$M^+$−H as intermediate, in which the metal (M) is oxidatively inserted in the R−H bond.[12] If we assume that both newly formed bonds in the inserted species have covalent character, R−$Mn^+$−H cannot originate from the septet ground-state asymptote of isolated $Mn^+$ ($^7S$) and RH. Consequently, for the manganese cation C−H and C−C bond activation will have to involve curve crossing from the high-spin entrance channel to intermediates with lower multiplicity. Indeed, in contrast to the ground state of $Mn^+$ ($^7S$), the excited $^5D$ and $^5S$ states react with alkanes, including C−C bond cleavage of ethane.[13] Although complexation energies upon formation of a metal−organic collision complex may be large enough to impel a spin conversion, as is hypothesized to occur in the reactions of the late transition-metal oxide cations with alkanes,[6b,c] in the case of bare $Mn^+$ the promotion energy is quite large. Thus, the energy gained upon complexation of alkanes is apparently not sufficient to render a transition state of lower multiplicity energetically accessible. For ground-state $Mn^+$, exothermic reactions have only been observed with *unsaturated* hydrocarbons as large as 4-octyne,[14] which exhibit much larger complexation energies than alkanes.[3]

It is well known in organometallic chemistry that ligand effects can be used to control the reactivity of metal compounds. With respect to gas-phase ion chemistry, previous studies have demonstrated that the oxide cations of the late first-row transition-metals Fe, Co, and Ni are much more reactive relative to their bare metal−ion analogues.[15-19] In particular, these $MO^+$ ions are able to oxidize $H_2$, methane, and benzene at thermal energies, whereas the corresponding bare metal ions do not react with these substrates.[3] Similarly, the reactivity of $CrO^+$ exceeds that of bare $Cr^+$; however, $CrO^+$ does not activate $H_2$ or $CH_4$.[20] In distinct contrast, for the early transition-metals Sc, Ti, and V the oxo ligand diminishes the reactivity of $MO^+$ relative to the bare metal ions $M^+$.[21,22] This is ascribed to the high oxophilicities of these early transition metals and high stabilities of the $M^+$−O multiple bonds, which render O-atom transfer from these oxides to organic substrates endothermic.[23,27] In addition, in these three systems the spin population of the oxygen atom is zero in contrast to, e.g., $MnO^+$.[27]

Most reports on the chemistry of $MnO^+$ primarily addressed its generation from bare $Mn^+$.[23,24] Stevens and Beauchamp reported that $MnO^+$ reacts with ethene to form $Mn^+$ and $MnCH_2^+$ with concomitant $C_2H_4O$ and $CH_2O$ eliminations, respectively.[25] Although this study indicated that $MnO^+$ is a viable oxidant in the gas phase, the reactivity of $MnO^+$ toward alkanes has not yet been examined. Moreover, $MnO^+$ has been suggested as a case in point for the principle of spin conservation in transition-metal ion chemistry.[21]

Here, we report the reactions of $MnO^+$ with molecular hydrogen, methane, and several small alkanes. In addition, we describe ab initio calculations for $MnO^+$ and $MnOH^+$, in order to evaluate energetics, structures, and electronic ground states as well as excited states of both ions. Finally, a qualitative model of the $MnO^+$/RH potential energy hypersurface (where R = H) will be presented and used to interpret the reactions of $MnO^+$ with larger substrates.

## Results and Discussion

**The $MnO^+$ Cation.** Although reaction 2 is exothermic by 29 kcal/mol,[23] the reaction must proceed via curve crossing to satisfy the symmetry requirements for the conversion of $Mn^+$ to $MnO^+$.[24b] Details concerning the generation and subsequent collisional thermalization of $MnO^+$ from laser-desorbed $Mn^{+*}$ with $N_2O$ have been described previously.[19d] Briefly, reaction

$$Mn^+ + N_2O \rightarrow MnO^+ + N_2 \quad (2)$$

2 was realized by kinetically exciting mass-selected $Mn^+$ with an appropriate low-energy rf pulse in the presence of $N_2O$. The extent of translational excitation is not unlimited because at high kinetic energies it will result in collisional induced dissociation (CID) of the product or even approach ion-ejection energies rather than ion activation; consequently, the absolute yield of $MnO^+$ will decrease although yields with respect to $Mn^+$ will increase. Therefore, a complete conversion of $Mn^+$ to $MnO^+$ was not achieved, since ion excitation, ion ejection, quenching processes, and conducting the reaction of interest compete with each other, and the optimal yield of $MnO^+$ amounts to ca. 30%

(11) The collision rate constants $k_C$ were calculated according to Su, T.; Chesnavich, W. J. *J. Chem. Phys.* **1982**, *76*, 5183.

(12) Besides the mechanisms described in this paper, there exists another pathway for C−H and C−C bond activation by transition-metal ions, namely the migratory insertion mechanism. For details, see: Huang, Y.; Hill, Y. D.; Sodupe, M.; Bauschlicher, C. W., Jr.; Freiser, B. S. *J. Am. Chem. Soc.* **1992**, *114*, 9106 and references cited therein.

(13) (a) Strobel, F.; Ridge, D. P. *J. Phys. Chem.* **1989**, *93*, 3635. For a review, see: (b) Armentrout, P. B. *Annu. Rev. Phys. Chem.* **1990**, *41*, 313.

(14) (a) Schulze, C.; Schwarz, H. *J. Am. Chem. Soc.* **1988**, *110*, 67. (b) Schulze, C.; Weiske, T.; Schwarz, H. *Organometallics* **1988**, *7*, 898. (c) Schulze, C.; Schwarz, H. *Int. J. Mass Spectrom. Ion Processes* **1989**, *88*, 291.

(15) (a) Jackson, T. C.; Jacobson, D. B.; Freiser, B. S. *J. Am. Chem. Soc.* **1984**, *106*, 1252. (b) Schröder, D.; Schwarz, H. *Angew. Chem., Int. Ed. Engl.* **1990**, *29*, 1431. (c) Schröder, D.; Schwarz, H. *Angew. Chem. Int. Ed. Engl.* **1991**, *29*, 1433. (d) Ref. 6. (e) Schröder, D.; Fiedler, A.; Ryan, M. F.; Schwarz, H. *J. Phys. Chem.*, **1994**, *98*, 68.

(16) Ryan, M. F.; Fiedler, A.; Schröder, D.; Schwarz, H. *Organometallics* **1994**, *13*, 4072.

(17) Ryan, M. F.; Schwarz, H., unpublished results.

(18) (a) Chen, Y.-M.; Clemmer, D. E.; Armentrout, P. B. *J. Am. Chem. Soc.* **1994**, *116*, 7815. (b) Clemmer, D. E.; Chen, Y.-M.; Khan, F. A.; Armentrout, P. B. *J. Phys. Chem.* **1994**, *98*, 6522.

(19) (a) Schröder, D.; Schwarz, H. *Helv. Chim. Acta* **1992**, *75*, 1281. (b) Schröder, D.; Florencio, H.; Zummack, W.; Schwarz, H. *Helv. Chim. Acta* **1992**, *75*, 1792. (c) Becker, H.; Schröder, D.; Zummack, W.; Schwarz, H. *J. Am. Chem. Soc.* **1994**, *116*, 1096. (d) Ryan, M. F.; Stöckigt, D.; Schwarz, H., *J. Am. Chem. Soc.* **1994**, *116*, 9565. (e) For an exhaustive review on this topic, see ref 6c.

(20) (a) Kang, H.; Beauchamp, J. L. *J. Am. Chem. Soc.* **1986**, *108*, 5663. (b) Kang, H.; Beauchamp, J. L. *J. Am. Chem. Soc.* **1986**, *108*, 7502.

(21) Clemmer, D. E.; Aristov, N.; Armentrout, P. B. *J. Phys. Chem.* **1993**, *97*, 544.

(22) Jackson, T. C.; Carlin, T. J.; Freiser, B. S. *J. Am. Chem. Soc.* **1986**, *108*, 1120.

(23) Fisher, E. R.; Elkind, J. L.; Clemmer, D. E.; Georgiadis, R.; Loh, S. K.; Aristov, N.; Sunderlin, L. S.; Armentrout, P. B. *J. Chem. Phys.* **1990**, *93*, 2676.

(24) (a) Kappes, M. M.; Staley, R. H. *J. Phys. Chem.* **1981**, *85*, 9421. (b) Armentrout, P. B.; Halle, L. F.; Beauchamp, J. L. *J. Chem. Phys.* **1982**, *76*, 2449.

(25) Stevens, A. E.; Beauchamp, J. L. *J. Am. Chem. Soc.* **1979**, *101*, 6449.

(26) Buijse, M. A.; Baerends, E. J. *Theoret. Chim. Acta* **1991**, *79*, 389.

(27) (a) Carter, E. A.; Goddard, W. A. *J. Phys. Chem.* **1988**, *92*, 2109. (b) It should be noted that, based on GVB + CI calculations, the Carter−Goddard paper (ref 27a) gives an excellent analysis on the bonding properties of $MO^+$ (M: first- and second-row transition-metal atom) and their implications for the oxidation capabilities of these diatomic oxides.

**Table 1.** Low-Lying Electronic States, Excitation Energies $\Delta E$ (kcal/mol), Bond Lengths $r$ (Å) for the Ground States of $MnO^+$ and $MnOH^+$, and Bond Dissociation Energies BDE (kcal/mol) to the Ground-State Dissociation Products $Mn^+$ ($^7S$), O ($^3P$), and HO• ($^2\Pi$), Respectively[a]

| species | state | $\Delta E$ | $r$(Mn−O) | $r$(O−H) | BDE |
|---|---|---|---|---|---|
| $MnO^+$ | $^5\Sigma^+$ | 0.0 | 1.59 | | 65.4[b] |
| | $^5\Pi$ | 1.9 | 1.58 | | |
| | $^7\Pi$ | 22.3 | 1.83 | | |
| | $^3\Delta$[c] | 65.8 | 1.51 | | |
| $MnOH^+$ [d] | $^6A'$ | 0.0 | 1.68 | 0.993 | 74.2[e] |
| | $^4A'$ | 80.1 | 1.67 | 1.002 | |
| | $^4A''$ | 80.8 | 1.65 | 1.004 | |

[a] Geometries optimized using the ADF density functional theory approach; the energetics refer to the CASPT2D level of theory (see computational details). [b] Experimental BDE($Mn^+$−O) = 68 kcal/mol; ref 23. [c] According to the DFT computations, the energetically lowest-lying triplet state of $MnO^+$ is much higher in energy than the states considered here, therefore, the triplet states were not examined further at the CASPT2D level of theory. [d] For the angle α(Mn−O−H) of $MnOH^+$, see text. [e] Bracketed experimental value for BDE($Mn^+$−OH) = 81 ± 4 kcal/mol; see text and ref 33.

based on the initial $Mn^+$ intensity. Subsequently, pulsed-in argon buffer gas (ca. 100 collisions) was used to thermalize the so-formed $MnO^+$ ions.[19d]

As far as the electronic ground state of $MnO^+$ is concerned, previous calculations[26] proposed a triple-bonded, closed-shell ion of $^1\Sigma^+$ configuration. However, qualitative theoretical considerations indicate already that this assignment is incorrect, and for $MnO^+$, quintet ground states ($^5\Pi$ or $^5\Sigma^+$) were suggested by Carter and Goddard[27] as well as Clemmer et al.,[21] being consistent with the description of other first-row transition-metal oxide cations.[6b,c] In order to address this question by means of quantitative arguments, we have studied $MnO^+$ computationally by using an approach which combines density functional theory (DFT)[28] with high-level ab initio molecular orbital methods (see computational details). In brief, the geometries of the various states of $MnO^+$ have been optimized using DFT, and subsequently, the order of relative stabilities of the energetically low-lying states have been computed at the CASPT2D level of theory.

According to our computational results for $MnO^+$ (Table 1), the $^5\Sigma^+$ and $^5\Pi$ states are very close both in energy and geometry ($\Delta E$ = 1.9 kcal/mol) with the $^5\Sigma^+$ being the electronic ground state of $MnO^+$. Considering the expected computational error at the level of theory applied, we cannot unambiguously assign which of the two states actually corresponds to the electronic ground state of $MnO^+$. However, states of other multiplicities, i.e., $^7\Pi$ and $^3\Delta$, are much higher in energy ($\Delta E$ = 22.3 and 65.8 kcal/mol, respectively) and are not likely to be involved in the chemistry of $MnO^+$. Consequently, the ground state of $MnO^+$ corresponds to a quintet state of either $^5\Sigma^+$ or $^5\Pi$ configuration. This assignment is in line with the $^5\Pi$ ground state of isoelectronic neutral CrO, and the quintet states arising for $MnO^+$, by formal removal of one electron either out of an antibonding $\pi$ or $\sigma$ orbital of the $^6\Sigma^+$ ground state of neutral MnO.[29] As far as the bond dissociation energy (BDE) of $MnO^+$ is concerned, our results at the CASPT2D level of theory assign a value of 65.4 kcal/mol. This computed BDE agrees quite well with the experimental value of 68 ± 3 kcal/mol.[23] However, we note in passing that the method applied here in general does not warrant such an accuracy in calculating BDEs of ionic transition-metal compounds.[30]

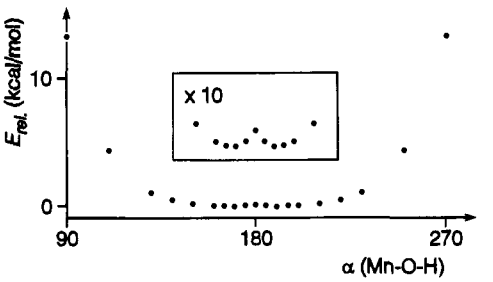


**Figure 1.** Energy profile of the bending mode of $MnOH^+$ ($^6A'$) at the CASPT2D level of theory (The Mn−O and O−H distances were kept frozen at the DFT-computed geometry).

As will be borne out in the following, $MnOH^+$ is an important species in the gas-phase chemistry of $MnO^+$. Qualitatively, $MnOH^+$ stems from either spin-coupling the 4s electron of $Mn^+$ ($^7S$) with an HO• radical, resulting in a $^6A'$ state, or by spin-coupling a quintet state of $MnO^+$ with H•, which leads to the $^4A'$ and $^4A''$ states, respectively. Therefore, only these sextet and quartet states of $MnOH^+$ were considered (Table 1). However, as it turned out in the calculations, the $^4A'$ and $^4A''$ quartet states are much higher in energy (>80 kcal/mol) as compared to the sextet $^6A'$ ground state of $MnOH^+$, and therefore, the low-spin states will not be pursued any further in the discussion. Interestingly, the potential energy hypersurface of $MnOH^+$ ($^6A'$) is rather flat with respect to the Mn−O−H bending mode. In fact, the DFT geometry optimization leads to a linear structure, whereas scanning of the Mn−O−H angle at the CASPT2D level of theory leads to a bent minimum structure with an Mn−O−H angle of ca. 170° (Figure 1). Obviously, the small energy difference of bent versus linear structures prevents a definitive decision of whether or not the $MnOH^+$ molecule is bent from being made; in particular, it is not clear whether the double minimum in Figure 1 will disappear upon further improving the level of theory used. Furthermore, if the effects of zero-point vibration are taken into account, the $MnOH^+$ ($^6A'$) will become quasilinear. For the $^6A'$ state of $MnOH^+$, the BDE($Mn^+$−OH) is calculated to be 74.2 kcal/mol, which is in reasonable agreement with the experimental values (see below).

**Reactions of $MnO^+$ with Dihydrogen, Methane, and Ethane.** Unlike the reactions of $FeO^+$, $CoO^+$, and $NiO^+$,[15,16,18] the reactivity of $MnO^+$ toward $H_2$ is high, and this metal-oxide cation reacts quite facile to eliminate $H_2O$ and H• as neutral products (Table 2). The pseudo-first-order rate constant for the $MnO^+/H_2$ couple amounts to $k_R = 2.3 \times 10^{-10}$ cm$^3$ molecule$^{-1}$ s$^{-1}$ and $k_R = 1.6 \times 10^{-10}$ cm$^3$ molecule$^{-1}$ s$^{-1}$ for the $MnO^+/D_2$ couple. Considering that the collision frequency for $H_2$ exceeds that of $D_2$ by a factor of 1.4, the reaction efficiencies $\Phi = k_R/k_C$ of both reactions are ca. 0.15, such that the intermolecular kinetic isotope effect (KIE)[31] associated with $H_2$ and $D_2$ oxidation is approximately unity.

From first-principle considerations, the occurrence of reaction 3 at thermal energies implies that BDE($Mn^+$−OH) must be larger than 70 kcal/mol.[32] This finding is consistent with a

$$MnO^+ + H_2 \rightarrow MnOH^+ + H^\bullet \qquad (3)$$

previous estimate of BDE($Mn^+$−OH) = 81 ± 4 kcal/mol, as derived from bracketing experiments, in which $MnOH^+$ is formed upon reaction of $MnO^+$ with R−H.[19d,33] According to

(28) Ziegler, T. *Chem. Rev.* **1991**, *91*, 651.
(29) Merer, A. J. *Annu. Rev. Phys. Chem.* **1989**, *40*, 407.
(30) Fiedler, A.; Hrušák, J.; Koch, W.; Schwarz, H. *Chem. Phys. Lett.* **1993**, *211*, 242.
(31) (a) Lewis, E. S. In *Isotope Effects in Organic Chemistry*; Buncel, E., Lee, C. C., Eds.; Elsevier: Amsterdam, 1976; p 127. (b) Derrick, P. J.; Donchi, K. F. In *Comprehensive Chemical Kinetics*; Bramford, C. H., Tipper, C. F. H., Eds.; Elsevier: Amsterdam, 1983; p 125. (c) Thibblin, A.; Ahlberg, P. *Chem. Soc. Rev.* **1989**, *18*, 209.

**Table 2.** Product Distribution for the Reaction of $MnO^+$ with $H_2$ and Selected Alkanes[a]

| | $Mn^+$ | $MnOH^+$ | $Mn(OH_2)^+$ | $(C_2H_4)MnOH^+$ | $(C_3H_6)MnOH^+$ | $(C_4H_8)MnOH^+$ | $(C_5H_{10})MnOH^+$ |
|---|---|---|---|---|---|---|---|
| $H_2$ | 25 | 75 | | | | | |
| methane | <1 | 100 | | | | | |
| ethane | 70 | 20 | 10 | | | | |
| propane | 55 | 20 | 10 | 15 | | | |
| *n*-butane | 30 | 15 | 30 | 10 | 15 | | |
| isobutane | 40 | 20 | 10 | | 30 | | |
| *n*-pentane | 25 | 15 | 25 | 10 | 13 | 12 | |
| isopentane | 25 | 30 | 20 | | | 25 | |
| neopentane | 5 | 20 | | | | 75 | |
| *n*-hexane | 20 | 10 | 35 | 10 | 10 | 10 | 5 |

[a] Distributions are listed as percentages of the total product-ion population.

this BDE($Mn^+$−OH) value, $\Delta H_R = -11$ kcal/mol results for reaction 3. We note in passing that BDE($Mn^+$−OH) = 81 ± 4 kcal/mol also agrees with an estimate that can be derived from the comparison of BDE($M^+$−F) and BDE($M^+$−OH) for M = Cr, Mn, and Fe: The BDE($M^+$−F) increases from 73 kcal/mol[32a] for M = Cr to 85 kcal/mol[32a] for M = Mn and 96 kcal/mol for M = Fe.[34] If we assume that a similar trend holds true for the metal hydroxide cations (BDE($M^+$−OH) of 73 kcal/mol[20] for M = Cr and 85 kcal/mol[35] for M = Fe), also an approximate value of ca. 80 kcal/mol for BDE($Mn^+$−OH) can be derived. Additional support for our bond dissociation energy estimate (Table 1) is obtained from the independent observation of ligand substitution reaction 4,[36] implying that the BDE($Mn^+$−OH) > 68 kcal/mol.

$$MnF^+ + H_2O \rightarrow MnOH^+ + HF \qquad (4)$$

As far as the reaction mechanism of $H_2$ activation by $MnO^+$ is concerned, the relatively large reaction efficiency, the preferred formation of $MnOH^+$, and the negligible intermolecular kinetic isotope effects indicate that the reaction of $MnO^+$ with $H_2$ can be explained by invoking a direct H-atom abstraction[38] as the initial step of the overall reaction sequence. Reaction 5, i.e., the highly exothermic formation of $Mn^+$ and water ($\Delta H_R = -50$ kcal/mol), needs a more complex scheme, since two O−H bonds are built up while the Mn−O bond breaks.

$$MnO^+ + H_2 \rightarrow Mn^+ + H_2O \qquad (5)$$

Before discussing this latter process, let us first recall the reactions of other transition-metal oxides with $H_2$. $FeO^+$ ($^6\Sigma^+$) reacts quite inefficiently with $H_2$ ($\Phi = 0.01$), although water elimination to yield $Fe^+$ ($^6D$) is a spin-allowed, exothermic process.[15e] This inefficiency has been attributed to the necessity of a spin−orbit coupling-mediated curve crossing as well as a multicentered transition-state which hinders the efficient formation of an H−$Fe^+$−OH insertion intermediate at low energies.[6b,18b] Similar arguments have been used to account for the inefficient reactions of $CoO^+$ and $NiO^+$ with $H_2$ ($\Phi \approx 10^{-3}$).[6b,18] If we apply these criteria to the reaction of $MnO^+$ ($^5\Sigma^+$, $^5\Pi$) with $H_2$, there is obviously no need for a curve crossing en route to the intermediate, since H−$Mn^+$−OH most likely exhibits a quintet ground state.[39] A qualitative potential energy hypersurface for reactions 3 and 5 is depicted in Figure 2.

As compared to other $MO^+/H_2$ systems, the fact that reaction 3 is exothermic for $MnO^+$ represents a fundamental difference as compared to other late transition-metal oxide cations. Consequently, in the ion/molecule reaction of $MnO^+$ ($^6A'$) with $H_2$, the encounter complex **1** and also the insertion intermediate **2** are rovibrationally excited to an extent that permits it to overcome the energy demand for dissociation into $MnOH^+$ and H•, i.e., the internal energy content of the intermediate is sufficient to induce direct bond cleavage. Therefore, within its lifetime excited **2** can rather be viewed as a pair of radicals, e.g. [H•/$MnOH^+$], **2′**, which can either directly dissociate (reaction 3) or, through a type of radical recombination process of the H atom and the OH group, reductively eliminate water via **3** (reaction 4). This scenario implies three important conclusions for the manganese system: First, the entrance energy level of $MnO^+ + H_2$ as compared to that of isolated $MnOH^+$ and H•, as well as the radicaloid nature of $MnO^+$, render a direct H-atom abstraction quite facile, where the hydrogen molecule approaches the oxygen terminus of $MnO^+$ asymmetrically. As exoergic H-atom transfer only requires activation of a single vibrational mode, facile H-atom transfer can occur, and **2′** can be generated from the reactants directly. Thus, even the encounter complex **1**, which is usually the first minimum along the potential energy hypersurface for R−H bond

(32) If not mentioned otherwise, additional thermochemical data were taken from the following: (a) Lias, S. G.; Bartmess, J. E.; Liebman, J. F.; Holmes, J. L.; Levin, R. D.; Mallard, W. G. *Gas Phase Ion and Neutral Thermochemistry*; American Institute of Physics: New York, 1988. (b) Berkowitz, J.; Ellison, G. B.; Gutman, D. *J. Phys. Chem.* **1994**, *98*, 2744. (c) $\Delta H_R$ values reported here include errors dependent upon the uncertainty of the literature data (ref 4, 5) and uncertainties resulting from the mixing of $\Delta H_f°$ values referenced at different temperatures. Corrections for $H_0° - \Delta H_T°$ have not been made.

(33) The previous value (ref 19d) has been refined using the salient data in ref 32b. This bracketing is also in good agreement with a previous value for BDE($Mn^+$−OH) = 82 ± 5 kcal/mol. See Clemmer, D. E.; Armentrout, P. B. In *NATO ASI Proceedings, Series C, Energetics of Organometallic Species*; Martinho Simões, J. A., Ed.; Kluwer: Dordrecht, 1992; Vol. 367, p 321.

(34) Schröder, D.; Hrušák, J.; Schwarz, H. *Helv. Chim. Acta* **1992**, *75*, 2215.

(35) BDE($Fe^+$−OH) has been determined repeatedly. The various values are in reasonable agreement with each other and range from 79 to 87 kcal/mol. For a discussion, see the following: (a) Reference 18b. (b) Marinelli, P. J.; Squires, R. R. *J. Am. Chem. Soc.* **1989**, *111*, 4101. (c) Magnera, T. F.; David, D. E.; Michl, J. *J. Am. Chem. Soc.* **1989**, *111*, 4100. (d) Dalleska, N. F.; Honma, K.; Sunderlin, L. S.; Armentrout, P. B. *J. Am. Chem. Soc.* **1994**, *116*, 3519.

(36) $MnF^+$ was generated in the reaction of $MnO^+$ with $C_6F_6$, and isolated $MnF^+$ was allowed to react with water to yield $MnOH^+$. For studies concerning the activation of C−F bonds (ref 37) by transition-metal cations, see: (a) ref 34. (b) Schröder, D.; Hrušák, J.; Tornieporth-Oetting, I. C.; Klapötke, T. M.; Schwarz, H. *Angew. Chem., Int. Ed. Engl.* **1994**, *33*, 212. (c) Heinemann, C.; Goldberg, N.; Tornieporth-Oetting, I. C.; Klapötke, T. M.; Schwarz, H. *Angew. Chem., Int. Ed. Engl.*, in press.

(37) Kiplinger, J. L.; Richmond, T. G.; Osterberg, C. E. *Chem. Rev.* **1994**, *94*, 373.

(38) For recent experimental and theoretical studies of H-atom abstraction by metal oxides, see: (a) Borve, K. J.; Petterson, L. G. M. *J. Phys. Chem.* **1991**, *95*, 3214. (b) Belyung, D.; Fontijn, A.; Marshall, P. *J. Phys. Chem.* **1993**, *97*, 3456. (c) Aray, Y.; Rodriguez, J.; Murgich, J.; Ruette, F. *J. Phys. Chem.* **1993**, *97*, 8398. Also see: (d) Tong, Y.; Lunsford, J. H. *J. Am. Chem. Soc.* **1991**, *113*, 4741.

(39) A quintet ground state for H−$Mn^+$−OH arises from spin coupling $MnOH^+$ ($^6A'$) with a hydrogen atom. Similarly, $(H_3C)_2Mn^+$ has a quintet ground state, see: Rosi, M.; Bauschlicher, C. W., Jr.; Langhoff, S. R.; Partridge, H. *J. Phys. Chem.* **1990**, *94*, 8656.

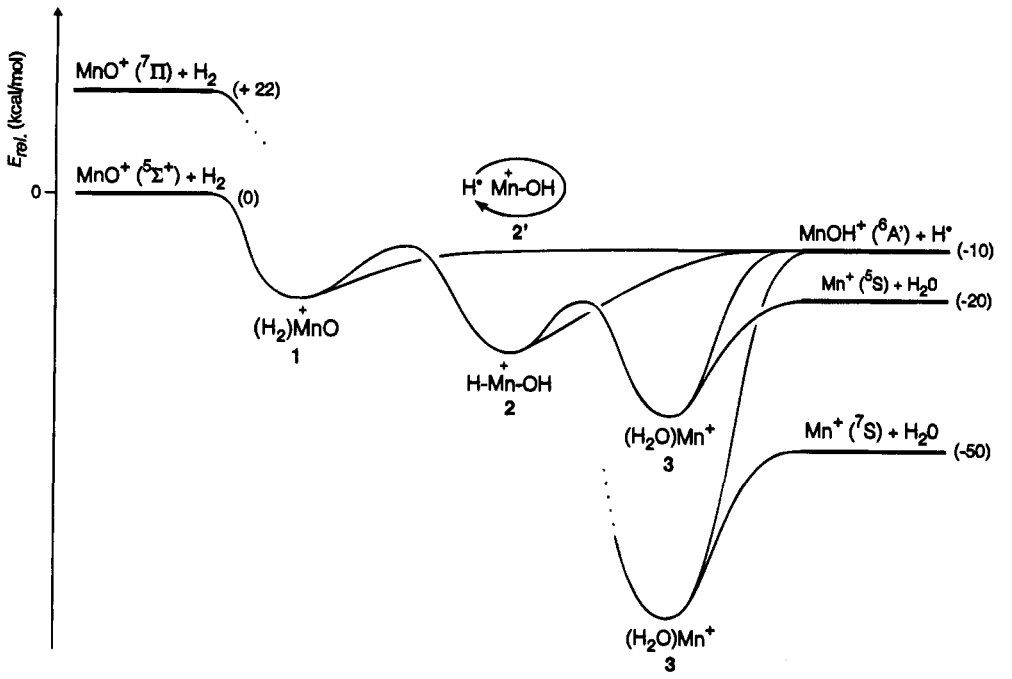


**Figure 2.** Schematic potential energy surfaces for the reactions of two electronic states of $MnO^+$ with $H_2$. The central barrier represents the conversion of a collision complex to an inserted intermediate. Values in parentheses are energy differences relative to the ground-state entrance channel in kcal/mol.

**Table 3.** Product Distributions for the Reaction of $MnO^+$ with $D_2$ and Selected Alkane Isotopologues[a]

| | $Mn^+$ | $MnOH^+$ | $MnOD^+$ | $Mn(OHD)^+$ | $(C_2H_2D_2)MnOH^+$ [b] | $(C_3H_5D)MnOH^+$ [b] |
|---|---|---|---|---|---|---|
| $D_2$ | 45 | 55 | | | | |
| $CH_2D_2$ | <1 | 65 | 35 | | | |
| $CD_4$ | <1 | | 100 | | | |
| $CH_3CD_3$ | 70 | 15 | 8 | 7 | | |
| $CH_3CD_2CH_3$ | 50 | 20 | 5 | 5 | 20 | |
| $(CH_3)_3CD$ | 40 | 20 | 5 | 2 | | 33 |

[a] Distributions are listed as percentages of the total product ion population. [b] These isotopologues are formed exclusively.

activation by $MO^+$,[6b] must not neccessarily be invoked in the mechanism for H—H bond activation by $MnO^+$. Second, the dissociative nature of the excited intermediate allows that H-atom loss, as well as water formation, can avoid reaction barriers of the type encountered in the reactions of the late transition-metal oxide cations with $H_2$.[6b,15e,16,18,21] However, for the manganese system a subsequent curve crossing to yield the ground-state products $Mn^+$ ($^7S$) and water may follow bond activation. This is due to the fact that the formation of the first electronically excited states $Mn^+$ ($^5S$ and $^5D$) is less probable on energetic grounds, and within experimental error the reactivity of $Mn^+$ being generated in reaction 5 is identical to that of the thermalized $Mn^+$ cations which served as precursors.[40] Overall, we can classify the $MnO^+$-mediated activation of $H_2$ as a reaction typical of an oxygen-centered radical, somewhat resembling Fenton chemistry in the condensed phase.[41,42]

As far as the branching ratios are concerned (Table 3), the channel for reductive elimination of water increases by nearly a factor of 2 upon going from $H_2$ to $D_2$, whereas the reaction efficiencies are similar. This effect is not entirely unexpected: While on the one hand isotopic substitution hinders bond activation, on the other hand the lifetime of rovibrationally excited intermediates will be larger for the deuterated species due to its higher density of states. Since the dissociation of **2'** is dependent upon its lifetime, the possibility of rearrangement and subsequent curve crossing to yield $Mn^+$ ($^7S$) and water will increase upon deuteration at the expense of $D^\bullet$ loss to yield $MnOD^+$. We note in passing that this interplay of kinetic isotope and lifetime effects becomes apparent here, since collisional stabilization of **1** or **2** is not possible in the low-pressure regime that pertains in these experiments, such that the probability of third-body collisions is negligible.[10]

For the sake of completeness, we note that $MnOD^+$ undergoes H/D exchange with background water to yield $MnOH^+$ (background pressure ca. $1 \times 10^{-9}$ mbar).[43,44] This process occurs rapidly, and at longer reaction times $MnOH^+$ becomes the most abundant ion in the spectrum. In addition, association to yield $MnOH(H_2O)^+$ was observed. For the evaluation of precise branching ratios, isotopic exchanges and condensation reactions were suppressed by using reagent pressures in large excess relative to the amount of background water.

(40) For reactions of excited $Mn^+$, see: (a) Strobel, F.; Ridge, D. P. *J. Phys. Chem.* **1989**, *93*, 3635. (b) Elkind, J. L.; Armentrout, P. B. *J. Chem. Phys.* **1986**, *84*, 4862. (c) Georgiadis, R.; Armentrout, P. B. *Int. J. Mass Spectrom. Ion Processes* **1989**, *91*, 123. (d) Sunderlin, L. S.; Armentrout, P. B. *J. Phys. Chem.* **1990**, *94*, 3589. It should be mentioned that in ref 40d it has also been pointed out that $Mn^+$ reactions may involve substantial radical character.

(41) Dobbs, K. D.; Dixon, D. A.; Komornicki, A. *J. Chem. Phys.* **1993**, *98*, 8852.

(42) Wong, W.-D.; Bakac, A.; Espenson, J. H. *Inorg. Chem.* **1993**, *32*, 2005.

(43) The background pressure in the mass spectrometer consists of water, air, and the residues from organic reagents. Thus, a precise $k_R$ estimate for H/D exchange of $MnOD^+$ with background water is not possible. However, assuming $p(H_2O) \approx 1 \times 10^{-9}$ mbar, the H/D exchange process is presumed to be essentially collisional.

(44) (a) Blum, O.; Stöckigt, D.; Schröder, D.; Schwarz, H. *Angew. Chem., Int. Ed. Engl.* **1992**, *31*, 603. (b) Schröder, D.; Hrušák, J.; Schwarz, H. *Ber. Bunsen Ges. Phys. Chem.* **1993**, *97*, 1085.

Scheme 1

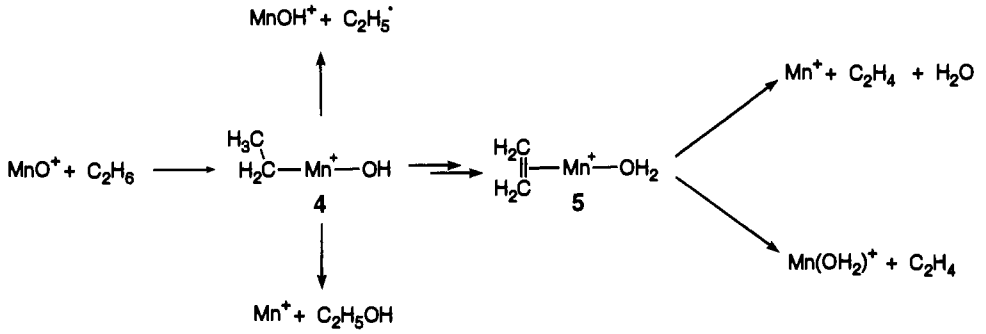


For the reaction of $MnO^+$ with methane (Table 2), the H-atom abstraction reaction (6) to form $MnOH^+$ is the most prominent process, with $\Delta H_R = -12$ kcal/mol.

$$MnO^+ + CH_4 \rightarrow MnOH^+ + CH_3^\bullet \qquad (6)$$

Interestingly, the $Mn^+$ cation is observed as a minor component. On thermochemical grounds, the neutral product of reaction 7 is presumed to be methanol ($\Delta H_R = -22$ kcal/mol). The rate for the oxidation of methane to methanol mediated by $MnO^+$ is estimated to be $k_R \approx 1 \times 10^{-11}$ cm$^3$ molecule$^{-1}$ s$^{-1}$ ($\Phi \approx 0.01$).

$$MnO^+ + CH_4 \rightarrow Mn^+ + CH_3OH \qquad (7)$$

When the reaction of $MnO^+$ with $H_2$ and $CH_4$ is compared, the branching ratios for H-atom abstraction and O-atom transfer to generate ROH change dramatically. More precisely, while 25% $H_2O$ is formed from dihydrogen, less than 1% $CH_3OH$ evolves from methane. This effect can be attributed to at least two origins: (i) There is a competition between radical loss and combined hydrogen transfer/reductive elimination processes, which reflects the significantly different exothermicities for $H_2O$ and $CH_3OH$ formations, respectively. Whereas for dihydrogen the process to yield water is highly exothermic ($\Delta H_R = -50$ kcal/mol), production of methanol from methane is associated with a much smaller exothermicity ($\Delta H_R = -22$ kcal/mol). (ii) As pointed out by a reviewer, the *directional* bonding of the sp$^3$-hybridized $CH_3$ species versus that of the *spherical* bonding of a hydrogen atom will favor hydrogen atom migration as compared with that of a methyl radical.

The operation of the H-atom abstraction mechanism is further supported by the reactions of $MnO^+$ with the methane isotopologues $CH_2D_2$ and $CD_4$ (Table 3). For example, the efficiency $\Phi$ for reaction 6 is 0.43 as compared to 0.40 for the $MnO^+/CH_2D_2$ couple and 0.37 for the $MnO^+/CD_4$ couple; thus, the intermolecular KIE of $k_H/k_D$ amounts to ca. 1.04 per D atom and is almost negligible. However, an *intramolecular*[31] KIE of $k_H/k_D$ ca. 2 can be established from the relative abundances of $MnOH^+$ and $MnOD^+$ for the reaction of $MnO^+$ with $CH_2D_2$. For comparison, an *intra*molecular KIE of 4.6 was established for the formation of $FeOH^+/FeOD^+$ from the $FeO^+/CH_2D_2$ couple.[15c] For $FeO^+$, an initial C–H bond activation to form an $CH_3$–Fe–$OH^+$ intermediate most likely occurs,[6] which can then expel $CH_3^\bullet$ or reductively eliminate methanol. Also, for the $FeO^+/CH_4$ couple, the reaction efficiency ($\Phi = 0.2$) is smaller than that for the $MnO^+$ system. The relatively large $\Phi$ value and the small *intra-* and *inter*molecular kinetic isotope effects of $MnO^+$ as compared to those of $FeO^+$ are consistent with the model depicted in Figure 2 for the reaction of $MnO^+$ with $H_2$.

Overall, $MnO^+$ reacts more efficiently with methane than any other first-row transition-metal oxide cations. The oxides of $Sc^+$ through $Cr^+$ are not observed to react with methane,[15] $CoO^+$ reacts with methane very slowly ($\Phi \approx 10^{-3}$),[16] and $NiO^+$ reacts with methane, exclusively via reductive elimination of methanol at an efficiency of $\Phi = 0.2$.[17] However, if only oxidation to methanol is considered, $MnO^+$ is inefficient as compared to $FeO^+$ and $NiO^+$. Nevertheless, it should be pointed out that the relative efficiencies within the first-row transition-metal series is in direct contrast to the association efficiency of the bare $M^+$ cations with methane ($\Phi < 10^{-4}$) relative to other first-row transition-metal cations.[10] Thus, the oxo ligand increases the reactivity of manganese cation by more than 4 orders of magnitude. This dramatic ligand effect can easily be accounted for in terms of electronic arguments: While the reactions of bare $Mn^+$ are hampered through the repulsive electron in the 4s orbital of the $^7S$ ground state, in $MnO^+$ this electron is involved in a strongly polarized bond to the oxygen atom, such that the antibonding $\sigma^*$ orbital of the Mn–O bond—which resembles the 4s orbital of $Mn^+$—is unoccupied.

For alkanes larger than methane, $\beta$-H transfer emerges as a new and facile decomposition process of the rovibrationally excited insertion intermediate **4** being formed via initial C–H bond activation (Scheme 1). Furthermore, increasing polarizabilities of higher alkanes and larger reaction exothermicities render the pseudo-first-order rate constants for the $MnO^+/C_2H_6$ couple, as well as for the other larger alkane systems, to become saturated at the collision frequency, i.e., $\Phi = 1$. The $Mn^+$ cation is the most abundant product ion in the reaction of $MnO^+$ with ethane. As indicated in Scheme 1, $Mn^+$ can result from two pathways: reductive elimination of ethanol from **4** or combined ethene/water loss from intermediate **5**. Estimates of $\Delta H_R$ for the elimination of ethanol, combined ethene/water losses, ethene, and ethyl radical formation for the $MnO^+$/ethane couple are −28, −17, −46, and −15 kcal/mol, respectively.[32] Since reductive elimination seldom occurs in the $MnO^+/CH_4$ system, and there exists no reason why this channel should be favored for ethane, $Mn^+$ production is more likely due to consecutive losses of ethene and water. The formation of the $Mn(H_2O)^+$ ion can be rationalized by the intermediacy of **5**, formed via $\beta$-H-atom transfer from **4**, which then preferentially eliminates an ethene ligand. The $Mn(C_2H_4)^+$ ion is not observed, perhaps due to the predicted low bond strength, $BDE°(Mn^+–C_2H_4)$ = 20 kcal/mol,[45] whereas $BDE°(Mn^+–OH_2)$ = 29 kcal/mol.[35b] The mechanism outlined in Scheme 1 is further supported by the formation of $Mn(HDO)^+$ in the reaction of $CH_3CD_3$ with $MnO^+$ (Table 3). Consecutive and rapid H/D exchange reactions of $Mn(OHD)^+$ and also of $MnOD^+$ with background water lead to a mixture of $Mn(H_2O)^+$ and $MnOD^+$ ions ($m/z$ = 73 for both ions). Therefore, the precise determination of kinetic

(45) Sodupe, M.; Bauschlicher, C. W., Jr.; Langhoff, S. R.; Partridge, H. *J. Phys. Chem.* **1992**, *96*, 2118 (Addendum **1992**, *96*, 5670).

**Scheme 2**

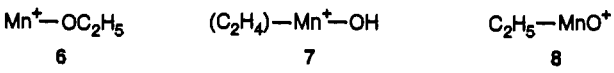


isotope effects associated with $MnOH^+$ and $MnOD^+$ formation is hampered in this experiment. While the mass separation of the isobaric multiplet is in general relatively straightforward in FTICR mass spectrometry, in the present case we are facing a dilemma: On the one hand, high-resolution FTICR experiments require low pressures and relatively long reaction times, on the other hand H/D exchange reactions with background water can only be avoided by high reagent pressures and short reaction times. Despite these complications, an estimate of an *intra*molecular KIE of $k_H/K_D \approx 2$ can be derived from the productions of $MnOH^+$ and $MnOD^+$ in the $MnO^+/CH_3CD_3$ system; this value is in agreement with the corresponding value derived from the $MnO^+/CH_2D_2$ couple. Apparently, the relative abundance of the $Mn(OHD)^+$ decreases upon deuteration as compared to the unlabeled case, while H-atom abstraction processes increase slightly. This effect of isotopic labeling on the product branching ratio can be due to either secondary kinetic isotope effects arising from the formation of neutral $CH_2{=}CD_2$ or primary kinetic isotope effects associated with C—H bond activation and subsequent $\beta$-H-atom transfer; however, the experimentally measured effect is too small to draw further conclusions.

**The Reaction of $MnO^+$ with Propane and Larger Alkanes.** In general, the reactions of $MnO^+$ with propane and larger hydrocarbons also proceed via initial C—H bond activation and elimination of neutral alcohols, olefins, and water (Table 2) and follow the mechanism outlined for the ethane system (Scheme 1). As far as the initial C—H bond activation step is concerned, for the reaction of $CH_3CD_2CH_3$ with $MnO^+$ after statistical correction of the ratio of $MnOH^+$ and $MnOD^+$ for the number of H/D atoms, a factor of 1.3 results. If one takes into account that a kinetic isotope effect is operative in C—D bond activation, this finding implies that that activations of primary and secondary C—H bonds in propane have similar probabilities. For the $MnO^+/(CH_3)_3CD$ system, the data clearly exhibit preferred activation of the tertiary C—H bond of *iso*butane, which is in keeping with the radicaloid nature of $MnO^+$.

Of interest for the larger systems is the observation of alkyl radical losses. Because of the complexity of the reactions for larger alkanes, as well as problematic H/D exchanges for the isotopic labeling studies as described above, we will focus on the $MnO^+$/propane system as a prototype. Furthermore, the reactions of the higher alkanes can completely be rationalized by using the mechanistic scenario which will be outlined for the reaction of $MnO^+$ with propane.

In the reaction of $MnO^+$ with propane, methyl radical loss leads to $[Mn, C_2, H_5, O]^+$, which may exhibit ethoxide structure **6**, that of olefin complex **7**, or correspond to organometal oxide **8** (Scheme 2). Ligand-exchange reactions of mass-selected $[Mn, C_2, H_5, O]^+$ strongly support the connectivity of **7**. For example, the secondary reaction of the $[Mn, C_2, H_5, O]^+$ product ion with water leads to $MnOH(H_2O)^+$, indicating the presence of an intact olefin substructure. Similarly, $[Mn, C_2, H_5, O]^+$ reacts with $C_2D_4$ to yield $[Mn, C_2, H, D_4, O]^+$ exclusively (reaction 8), and ligand exchange of the ethene ligand for an isobutene ligand was also observed. This is precisely what one expects for **7**, whereas the metal alkoxide[46] **6** should primarily react via hydride transfer reactions, and **8** should undergo sequential H/D exchanges with $C_2D_4$ as well as oxidation reactions; however, none of these latter reactions are observed.

(46) Schröder, D.; Schwarz, H. *Angew. Chem., Int. Ed. Engl.* **1990**, *29*, 910.

**Scheme 3**

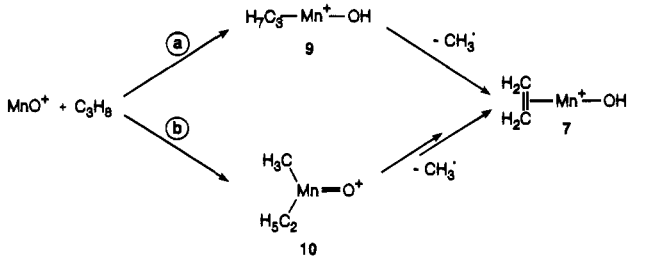


$$(C_2H_4)MnOH^+ + C_2D_4 \rightarrow (C_2D_4)MnOH^+ + C_2H_4 \quad (8)$$

Formation of the ($\eta^2$-olefin)$MnOH^+$ structure implies at least two different reaction mechanisms (Scheme 3). Either the reaction commences with the activation of a primary C—H bond to yield the inserted species **9** which subsequently undergoes radical homolysis (path **a**) or C—C bond activation may occur to yield **10** which may eventually lose a methyl radical, as proposed by Freiser and co-workers[15a] for the reaction of $FeO^+$ with larger alkanes (path **b**). Based on the experimental findings, we cannot unambiguously distinguish between both mechanisms; however, the fact that C—H bond activation seems to be the preferred reaction mode of $MnO^+$ points to the operation of mechanism **a**. In addition, intermediate **10** is not an ideal candidate for $CH_3^\bullet$ loss, since it involves an unfavorable high oxidation state for manganese. Also, $CH_3^\bullet$ loss from **10** would lead to the ethylmanganese oxide cation **8**; a structure which can be ruled out as it is not compatible with the ligand-exchange reactions described above. In addition, the absence of the $(C_2H_4)MnOH^+$ cation in the reaction of $MnO^+$ with ethane can easily be rationalized by the fact that $H^\bullet$ loss from an ethyl group would be 14 kcal/mol energetically more demanding than $CH_3^\bullet$ loss from larger alkanes (reactions 9).

$$C_2H_5^\bullet \rightarrow C_2H_4 + H^\bullet + 37 \text{ kcal/mol} \quad (9a)$$

$$C_3H_7^\bullet \rightarrow C_2H_4 + CH_3^\bullet + 23 \text{ kcal/mol} \quad (9b)$$

The reactions of $MnO^+$ with branched alkanes studied here lead to the exclusive elimination of $CH_3^\bullet$ as the only alkyl radical (Table 2). Consequently, in the reaction of $MnO^+$ with branched alkanes C—C skeletal rearrangements do not occur during the lifetime of the collision complex. Of interest is that in the reaction of $MnO^+$ with $(CH_3)_3CD$, $[Mn, C_3, H_6, D, O]^+$ ion is formed concomitantly with $CH_3^\bullet$ loss. The ligand-exchange reaction of this ion with $H_2O$ yields $MnOH(H_2O)^+$, which supports a $(C_3H_5D)MnOH^+$ structure, similar to **7**. Thus, the $CH_3^\bullet$ elimination commences by attacking a *primary* C—H bond rather than the *tertiary* one. However, as mentioned above, from the reactions with the labeled and unlabeled isobutanes, it follows that H-atom abstraction to generate $MnOH^+$ and $C_4H_9^\bullet$ ensues mainly from a tertiary carbon. Finally, in the reactions of *n*-pentane and *n*-hexane, also ethyl and propyl radicals are lost, such that not only C—H bond activation in general but also this radical expulsion mediated by $MnO^+$ does not exhibit a distinct regioselectivity.

## Conclusions

$MnO^+$ can be generated by reacting kinetically excited $Mn^+$ with $N_2O$ as O-atom donor. Molecular orbital calculations at the CASPT2D level of theory reveal that $MnO^+$ exhibits a quintet ground state (either $^5\Sigma^+$ or $^5\Pi$), whereas the triplet and

heptet staes are significantly higher in energy.[47] The $MnOH^+$ cation which is formed in the reaction of $MnO^+$ with hydrocarbons has a $^6A'$ ground state. As a consequence, direct H-atom transfer from a substrate RH to $MnO^+$ is not subject to either spin or symmetry restrictions.

Manganese oxide cation reacts efficiently with dihydrogen, methane, and small alkanes via exoergic initial C−H bond activation. An asymmetric H-atom abstraction mechanism to form an $R-Mn-OH^+$ intermediate (R = H, alkyl) is used to rationalize product formations and is consistent with the general mechanism proposed for the reaction of $MnO^+$ with $H_2$. The so-formed rovibrationally excited intermediates can then decompose by elimination of either closed- or open-shell neutral species. In general, the chemistry of $MnO^+$ can be described as being dominated by radical abstraction processes. Once the carbon skeleton is large enough, the formation of the (olefin)-$MnOH^+$ complexes occurs via radical homolysis during the lifetime of the intermediates.

*As compared to the other first-row transition metals, $Mn^+$ is the least reactive toward alkanes, whereas $MnO^+$ is the most reactive metal oxide cation.* Unlike the situation for the late-transition-metal oxide cations, a curve-crossing process at the exit channel seems to be operative in the generation of $Mn^+$ from $MnO^+$ and dihydrogen and alkanes, respectively.

## Experimental and Computational Details

Gas-phase experiments were performed by using a Spectrospin CMS 47X Fourier-transform ion-cyclotron resonance mass spectrometer, which is equipped with an external ion source and which has been described in detail elsewhere.[48] Manganese cations were generated from laser desorption/ionization by focusing the beam of a Nd:YAG laser (Spectron Systems; $\lambda$ = 1064 nm) at a solid manganese target. The metal cations were transferred from the external ion source to the analyzer cell by a system of electrostatic potentials and ion lenses. Ions of interest were isolated by using FERETS,[49] a computer-controlled ion-ejection protocol which combines single-frequency ion-ejection pulses with frequency sweeps to optimize ion isolation. All functions of the instrument, including all pulse sequences, were controlled by a Bruker Aspect-3000 minicomputer. Details concerning the production and subsequent thermalization of $MnO^+$ cations have been previously described.[19d]

Pressures were measured by an ion gauge (Lambert) and corrected as previously described.[50,51] Pseudo-first-order rate constants reported in this study were determined from the logarithmic decay of reactant intensity over time and are reported with ±30% error. Branching ratios were derived from the analysis of the temporal product distributions and are reported with ±10% error.

The labeled reagents [$D_4$]methane (99 atom % D; MSD), [$D_2$]methane (98% D; Cambridge Isotopes), $D_2$ (99.5% D; Linde), and $CH_3CD_2CH_3$ (98 atom % D; Cambridge Isotopes) were used as supplied. $CH_3CD_3$ and $(CH_3)_3CD$ were prepared by hydrolyzing the appropriate Grignard reagents with either $H_2O$ or $D_2O$.[51] Other reagents were obtained in high purity from commercial sources and used as supplied.

Computational studies of $MnO^+$ and $MnOH^+$ were performed by combining density functional theory (DFT)[52] with high-level ab initio theory; the full details of this 2-fold approach and its reliability have been described in previous studies from our laboratory.[53] In brief, geometries of the various electronic states of $MnO^+$ and $MnOH^+$ were optimized using the ADF[54] suit of programs. For the DFT calculations we applied the local density functional of Vosko, Wilk, and Nusair,[55] the nonlocal gradient corrections for the exchange part as proposed by Becke,[56] and Perdew's nonlocal gradient corrections for correlation.[57] The valence electrons were described by double-$\zeta$ STO basis sets (4s, 3d, 4p on the metal, 2s, 2p on the oxygen, and 1s on the hydrogen atom, respectively), and the inner electrons were treated by the frozen-core approximation.

Subsequently, the energetically low-lying roots in all spatial and spin symmetries of $MnO^+$ and $MnOH^+$ were computed at the CASPT2D[58] levels of theory using the following atomic natural orbital (ANO) basis sets: (14s9p4d3f)/[5s4p3d2f] for oxygen, (8s4p3d)/[3s2p1d] for hydrogen, and (21s15p10d6f4g)/[8s7p6d4f2g] for manganese.[59] The CAS calculations were performed using the MOLCAS-2 package.[60] The active space consists mostly of the 4s and 3d orbitals of manganese, the 2s and 2p orbitals of oxygen, and the 1s orbital of hydrogen, respectively. All electrons were correlated at the CASPT2D level of theory. Bond dissociation energies were derived from the sum of the energies of the isolated molecules. All computations were performed on either IBM/RS 6000 workstations or a CRAY-YMP computer.

**Acknowledgment.** Financial support by the Deutsche Forschungsgemeinschaft, the Volkswagen-Stiftung, and the Fonds der Chemischen Industrie is appreciated. We are indebted to Professor P. B. Armentrout for providing us with preprints of his group's work concerning the chemistry of $FeO^+$ and $CoO^+$, Professor S. Shaik for enlightening discussions, and the reviewers for helpful comments.

JA9429982

(47) A reviewer has pointed out that the electronic structures of these two quintet states of $MnO^+$ are quite different. While $^5\Sigma^+$ exhibits a $\Pi$ electronic configuration similar to that in $O_2$ and in $MO^+$ (M = Fe, Co, Ni; see ref 6b), the $\Pi$ electronic structure of the $^5\Pi$ state resembles that of the $CrO^+$ ground state. In view of the fact that $CrO^+$ does not activate RH molecules (R = H, $CH_3$), ref 20, while $MO^+$ (M = Mn, Fe, Co, and Ni) do react with RH, one would expect that the $^5\Sigma^+$ state is responsible for the reactivity of $MnO^+$ as reported in the present work.

(48) (a) Eller, K.; Schwarz, H. *Int. J. Mass Spectrom. Ion Processes* **1988**, *83*, 23. (b) Eller, K.; Zummack, W.; Schwarz, H. *J. Am. Chem. Soc.* **1990**, *112*, 621.

(49) Forbes, R. A.; Laukien, F. H.; Wronka, J. *Int. J. Mass Spectrom. Ion Processes* **1988**, *83*, 23.

(50) Bartmess, J. E.; Georgiadis, R. M. *Vacuum* **1983**, *33*, 149.

(51) Schröder, D. Ph.D. Thesis, Technische Universität Berlin, Germany, D83, 1993.

(52) Ziegler, T. *Chem. Rev.* **1991**, *91*, 651.

(53) (a) Schröder, D.; Fiedler, A.; Schwarz, J.; Schwarz, H. *Inorg. Chem.* **1994**, *33*, 5094. (b) Reference 6b. (c) Also see: Schröder, D., Fiedler, A.; Schwarz, H. *Int. J. Mass Spectrom. Ion Processes* **1994**, *134*, 239. (d) Hrušák, J.; Schröder, D.; Schwarz, H. *Chem. Phys. Lett.* **1994**, *225*, 416.

(54) ADF package available from te Velde, G.; Baerends, E. J. Department of Theoretical Chemistry, Vrije Universiteit, Arnsterdam, Netherlands.

(55) Vosko, S. J.; Wilk, L.; Nusair, M. *Can. J. Chem.* **1980**, *58*, 1200.

(56) Becke, A. D. *Phys. Rev.* **1988**, *A38*, 2398.

(57) Perdew, J. P. *Phys. Rev.* **1986**, *B33*, 8822 (Erratum **1986**, *B34*, 7406).

(58) Andersson, K.; Malmqvist, P.-A.; Roos, B. O.; Sadlej, A. J.; Wolinski, K. *Phys. Chem.* **1990**, *94*, 5483.

(59) (a) Widmark, P.-O.; Malmqvist, P.-A.; Roos, B. O. *Theoret. Chim. Acta* **1991**, *77*, 291. (b) Pou-Amerigo, R.; Merchan, M.; Widmark, P.-O.; Roos, B. O., manuscript in preparation.

(60) Andersson, K.; Fülscher, M. P.; Lindh, R.; Malmqvist, P.-A.; Olsen, J.; Roos, B. O.; Sadlej, A. J.; MOLCAS version 2, University of Lund: Widmark, P. O., IBM, Sweden.